International Journal of Advanced Structural Engineering
a SpringerOpen Journal

ORIGINAL RESEARCH Open Access

Minimum depth of soil cover above long-span soil-steel railway bridges

Morteza Esmaeili[1*], Jabbar Ali Zakeri[1] and Parisa Haji Abdulrazagh[2]

Abstract

Recently, soil-steel bridges have become more commonly used as railway-highway crossings because of their economical advantages and short construction period compared with traditional bridges. The currently developed formula for determining the minimum depth of covers by existing codes is typically based on vehicle loads and non-stiffened panels and takes into consideration the geometrical shape of the metal structure to avoid the failure of soil cover above a soil-steel bridge. The effects of spans larger than 8 m or more stiffened panels due to railway loads that maintain a safe railway track have not been accounted for in the minimum cover formulas and are the subject of this paper. For this study, two-dimensional finite element (FE) analyses of four low-profile arches and four box culverts with spans larger than 8 m were performed to develop new patterns for the minimum depth of soil cover by considering the serviceability criterion of the railway track. Using the least-squares method, new formulas were then developed for low-profile arches and box culverts and were compared with Canadian Highway Bridge Design Code formulas. Finally, a series of three-dimensional (3D) finite element FE analyses were carried out to control the out-of-plane buckling in the steel plates due to the 3D pattern of train loads. The results show that the out-of-plane bending does not control the buckling behavior of the steel plates, so the proposed equations for minimum depth of cover can be appropriately used for practical purposes.

Keywords: Soil-steel bridge, Railway bridges, Large span, Finite element analysis, Minimum cover depth, Serviceability criterion

Introduction

Soil-steel bridges are categorized as composite structures and are composed of corrugated steel plates buried in engineered soil materials. One of the failure modes for these bridges can be initiated by shear or tension failure in the soil cover and can result in structural buckling due to an inadequate depth of soil above the metal structure. This mode of failure is often avoided in the design codes by specifying a minimum depth of soil cover.

The minimum depth of soil cover that has been used for soil-steel railway bridges by various codes such as the California Transportation System (*S*/5) CALTRANS (2000), British Design manual (*S*/5) DMRB (2001), American Iron and Steel Institute (*S*/4) CSPI and AISI (2002), and American Association of State Highway and Transportation Officials (*S*/5) (AASHTO Highway Bridges 2000) was originally empirical and defined by a fraction of the bridge span (*S*). Additionally, ASTM A796 introduced the minimum depth of cover, $H_{\min}$, as $H_{\min} = 0.55S\sqrt{(\mathrm{AL})d/EI}$, which depends on the *S*, axle load (AL), eccentric distance (*d*), elastic modulus (*E*), and the moment of inertia (*I*) of the corrugated steel plates (ASTM 1982). The Australian Rail Track Corporation (ARTC 2005) also recommended specific values for the minimum depth of cover for different classes of railway tracks.

However, in the OHBDC (1992), the empirical formulas for the depth of cover were modified based on the results of a finite element (FE) analysis that considered the geometric shape of the metal structure and the axle load of a truck (Hafez and Abdel-Sayed 1983). Furthermore, the minimum required depth of cover $H_{\min}$ in the third edition of the OHBDC (1992) and in the current Canadian Highway Bridge Design Code (CHBDC 2006) has been specified as the greater of 0.6 m or $D_h/6$ $((D_h/D_v)^{0.5})$ with a maximum of 1.5 m, where D_h and D_v are

* Correspondence: m_esmaeili@iust.ac.ir
[1]School of Railway Engineering, Iran University of Science and Technology, University Street, Hengam Aveneu, Narmak, Tehran 1684613114, Iran
Full list of author information is available at the end of the article

the effective span and rise of the metal structure, respectively CSPI and AISI (2002; CHBDC 2006). This empirical-based formula is commonly used to calculate the depth of cover for highway and railway bridges (Abdel-Sayed and Salib 2002; Hafez 1981). An analytical formula has not yet been established specifically for the minimum cover depth of railway bridges although several structural studies have been done on dynamic and static behaviors of soil-steel structures (Flener et al. 2005; Flener and Karoumi 2009; Manko and Beben 2005; Manko and Beben 2008).

The minimum depth of cover criterion was fundamentally developed to avoid problems associated with soil failure above the crown of a soil-steel bridge (Mohammed et al. 2002). Although this criterion may be sufficient for the serviceability of highway bridges, some revisions may be essential for railway bridges (due to heavier axle loads and relevant dynamic effects), especially for long-span conditions (Peck and Peck 1984). On the other hand, the serviceability and the riding comfort criteria for railway bridges have remarkable importance compared with highway bridges. From the structural design aspect of long-span railway bridges, the critical sections must be stiffened either by stiffening metal sheets or by utilizing sandwich panels as concrete-filled metal sections. The serviceability criteria of the soil-steel railway bridges with spans larger than 8 m that use stiffened panels have not been previously examined and are the main subject of this paper. Therefore, for this study, the CHBDC (2006) equations for minimum cover depth were modified to define the minimum required cover depth for railway bridges based on the two-dimensional (2D) and three-dimensional (3D) FE analysis results using the well-known PLAXIS codes for the aforementioned cases.

Regarding the special serviceability criteria for railway bridges, for computing the minimum depth of cover, the permissible settlement of the railway track and the buckling of the conduit walls in different sections along the longitudinal axis of the bridges in 3D analyses were controlled. For these cases, the spans from 8.07 up to 13.46 m of box culverts and 14.13 up to 23.40 m of low-profile arches using stiffened and non-stiffened deep corrugated panels have been considered.

This study assumes that all the metal structures are buried in well-graded gravel (GW) as engineered backfill material. The material nonlinearity of the soil and metal structure as well as the stage construction effects were accounted for in the numerical analyses, and the railway load model LM71 CEN (2002) has been applied.

The purpose of this study is to reexamine the equations of minimum cover depth of soil-steel railway bridges based on best-fitted curves of the numerical results of the 2D FE analyses. Thereafter, the results are compared with the values obtained from the CHBDC (2006) method.

Methods

The primary subject of the current study is to introduce a new set of minimum soil cover equations for long-span railway bridges based on the numerical interpolation of the results of the 2D FE analyses. These equations relate the minimum depth of cover to the relative stiffness of backfill and the culvert structures and effective span of the railway bridges.

To determine the variation trend of the minimum depth of cover along with its governing parameters (geometry, length of span, and the panel stiffness) through numerical analyses, the permissible settlement of the track, metal structure buckling, and soil body failure criteria have been checked initially for each bridge structure for a 0.6-m depth of cover (the minimum limit of cover depth specified by CHBDC). When all of the defined criteria have not been fulfilled simultaneously, the depth of soil cover above the crown was increased, and the analyses were then restarted for a new depth of cover. The minimum depth of cover in which all of the criteria were simultaneously fulfilled was chosen as the *minimum depth of soil cover* for a specific bridge structure.

In this manner, the results of the 2D FE analyses present specific patterns for the calculation of the minimum depth of cover for box culverts and low-profile arches. In order to check the applicability of the proposed equations for minimum depth of cover in practical problems, a series of 3D finite element analyses with more realistic idealization of the railway superstructure components and the lateral slope of bridge embankment were carried out to control the out-of-plane buckling in the steel plates.

The concept of using 2D and 3D FE analyses to determine the pattern of the minimum depth of cover for soil-steel railway bridges is shown in the flowchart of Figure 1.

Procedure of the numerical modeling

In this section, the numerical modeling specifications and the assumptions used in the analyses will be explained in detail. This explanation details the various aspects of numerical modeling such as the model geometry and boundary conditions, material properties, loading pattern, and monitoring of the desired results.

Model geometry and boundary conditions

Because the box and low-profile arch geometries of soil-steel railway bridges are commonly used for road or highway underpasses Planning and Budget Organization (1985), for this study, the geometry with four various spans were selected for the 2D and 3D analyses. The goal was to model the actual shape of the soil-steel railway bridges. Detailed dimensions of the bridges are

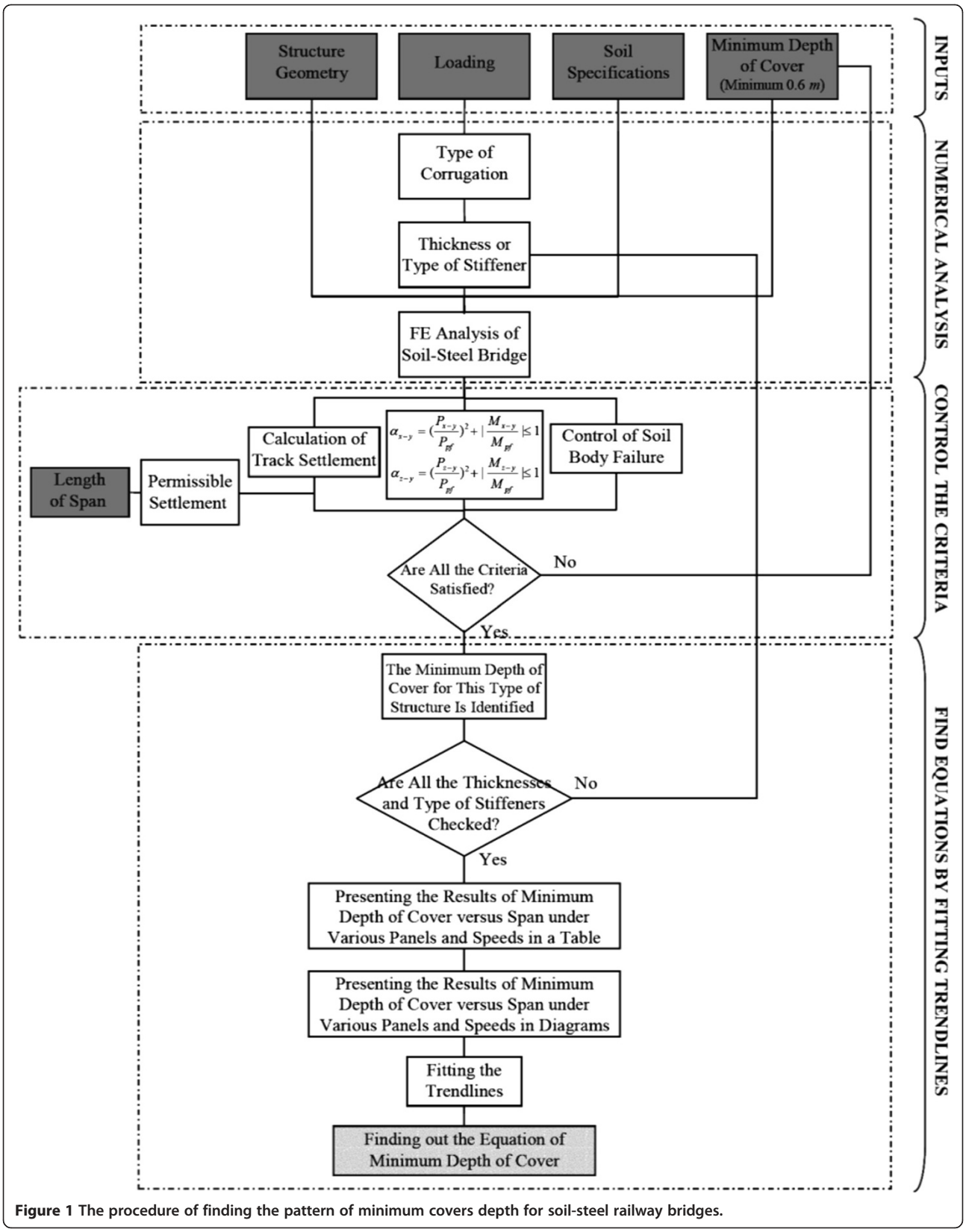

Figure 1 The procedure of finding the pattern of minimum covers depth for soil-steel railway bridges.

shown in Table 1 and Figure 2 Planning and Budget Organization (1985).

Two-dimensional idealization

Two-dimensional idealization was initially used wherein a transverse slice of unit length of the structure was assumed to be in a state of plane strain. In a plane-strain idealization, deformations perpendicular to the plane of the idealized structure are assumed to be zero.

The continuum media around the structure were extended to a triple distance of the outer side of the foundations in width for each side of the structure and four times of the total height of the structure by considering the minimum depth of cover beneath the structure. Standard fixities were applied as boundaries to the outer surfaces of the continuum media (see Figure 3). The vertical displacements are not fixed in vertical boundaries, but all displacements and rotations are fixed in the bottom boundary. These boundaries were specified after several analyses to minimize the effects of the boundaries on the results and geostatic pressures.

Because a large number of calculations (considering geometry and panel types, different depth of cover, axle loads, and loading patterns) were required to determine the preliminary new pattern of the minimum depth of cover, a 2D idealization was initially used to reduce the computing power and time required to perform the analyses. A 3D idealization was then used to control the out-of-plane buckling in the corrugated steel plates, to check the applicability of the 2D-based equations of minimum cover in practical 3D problems.

Three-dimensional idealization

As in practice, the train loading pattern has a 3D nature, so the derived values of minimum depth of soil cover based on 2D finite element analyses should be rechecked to consider the relevant 3D effects. These effects remarkably relates to the realistic load distribution pattern in railway superstructure as well as substructure components and the out-of-plane buckling modes of the steel plates. Consequently, the 3D numerical modeling of the selected structures was taken into consideration.

To reduce the computational costs in the 3D idealization, only half of the structure was modeled, which takes advantage of the symmetry of the railway cross section and loading pattern. Considering the assumed depth of the soil cover (1.5 m of covering material including the ballast and embankment layers) and a slope of 1 vertically to 1.5 horizontally of the ballast shoulders, the longitudinal dimension of each bridge was modeled. The 3D mesh was created using railway cross-sectional segments along the longitudinal axis of each structure.

For the 3D model, the boundaries were defined as 60 m in width from each side of the centerline of the structure and 60 m in depth from the underneath of foundation (see Figure 3). As in the 2D idealization, standard fixtures were applied as boundaries to the outer surfaces of the continuum media, and the boundaries were specified after several analyses to minimize the effects of the boundaries on the results and geostatic pressures.

The sequence of placing the engineering fill layers was presented in the 2D and 3D models. Therefore, each layer of the FE mesh was constructed sequentially. Because the actual number of layers employed in the placement of the backfill in a typical soil-steel bridge is too large to be conveniently used in the FE analyses, a smaller number of layers were used in the simulation of the construction process Abdel-Sayed et al. (1993).

Types of elements

To analyze the soil-steel railway bridge as a soil-structure interaction problem, two types of elements were defined in the solution process. The first group that deals with the structural elements such as the conduit

Table 1 Categories of the dimensions and use of the clearance boxes under low-profile arches and box culverts

	Box culvert	Low-profile arch
Span × Rise (Use of the clearance box under the structure)	8.07 m × 3.06 m	14.13 m × 5.37 m
	(Common for two-line local roads with minimum width)	(Common for two-line roads without considering the future development with ideal width)
	10.51 m × 3.55 m	16.52 m × 5.33 m
	(Common for two-line local roads with ideal width)	(Common for two-line main roads with considering the future development with minimum width)
	11.02 m × 3.24 m	20.95 m × 6.64 m
	(Common for two-line roads without considering the future development with minimum width)	(Common for developed four-line main road with minimum width)
	13.46 m × 3.49 m	23.40 m × 6.44 m
	(Common for two-line roads without considering the future development with ideal width)	(Common for developed four-line main road with ideal width)

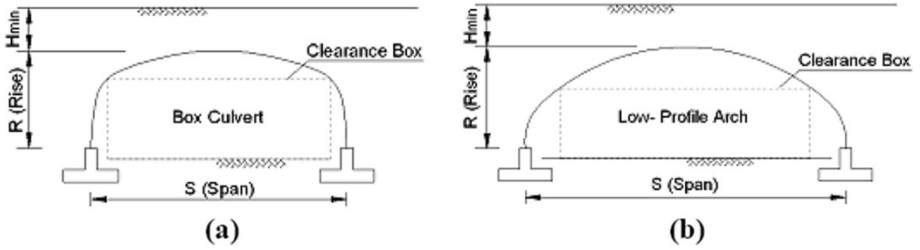

Figure 2 Clearance boxes under (a) box culverts and (b) low-profile arches.

walls and foundation system was introduced as beam elements and plate elements for the 2D and 3D FE modeling. The rails, which were idealized only in the 3D FE analysis, were modeled using plate elements.

For the second group that was used to idealize the engineered backfill, natural ground, and ballast material, 15-node triangular isotropic elements were used in the 2D analysis to have more accuracy results in the evaluation of stress and strain. On the other hand, for the 3D analysis, 15-node wedged elements were used to model the soil environment as well as the ballast and sleepers.

Full-bonded conditions are considered between materials in 2D and 3D FE analyses which cause more conservative results due to greater stresses induced in metal structures. On the other hand, the studies performed by Duncan (1979), MacDonald (2010), and Peterson et al. (2010) demonstrated that, in most cases, the effects of slip between the metal structure and the backfill is ignorable.

Material properties

Because of the serviceability and the riding comfort criteria for railway bridges, the critical sections are often stiffened either by stiffening metal sheets or by utilizing sandwich panels as concrete-filled metal sections. Because of obvious difference between the geometrical shape of the box and low-profile arch (LPA) types of the bridges, the initial analysis results show that for box and LPA, the critical sections are in the haunches and in the midspan, respectively.

The rigidity effects of the panels on the minimum depth of cover were examined using non-stiffened and stiffened panels of deep corrugations (Figure 4) for each of the structures. The panels were idealized as elasto-plastic beams or plates for the 2D and 3D FE idealizations. For the special case of the composite panel type VI, the cracked moment of inertia of the section was considered in the numerical calculations. The equivalent parameters of the beam which represents the corrugated profile are calculated based on the model of El-Sawy (2003). A summary of the parameters such as the axial stiffness (EA), the flexural rigidity (EI), the Poisson's ratio (v), the plastic moment capacity (M_p), and the compressive strength (P_p) for various types of panels are shown in Table 2 (Abdulrazagh 2009).

The behavior of the soil-steel bridge foundation and pedestals was idealized as elastic beams for the 2D analyses and as elastic plates for the 3D FE analyses, which

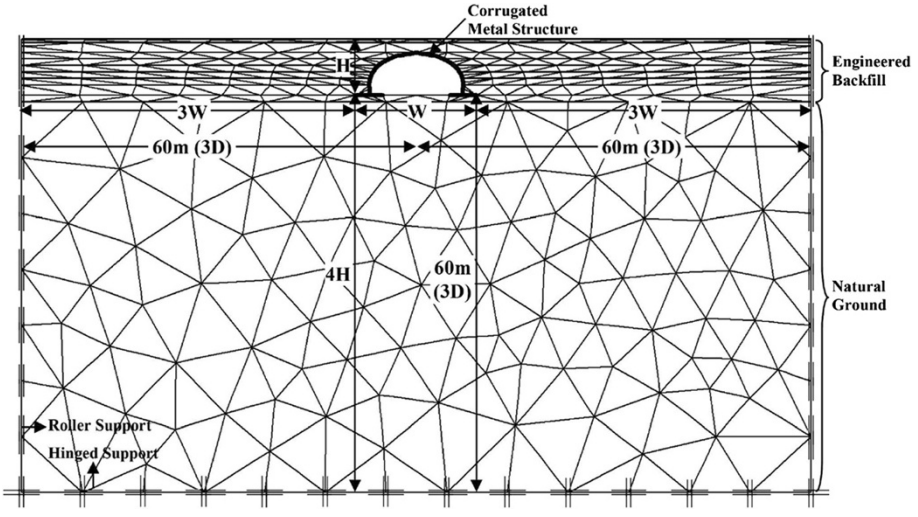

Figure 3 Finite element models (2D and 3D).

was used to maintain the elastic characteristics under load. This was assumed because the initial studies on the behavior of the foundation system demonstrated that, for the design specifications of the foundation system and under the conditions used for this study, the foundation and pedestals did not exhibit a considerable amount of nonlinear behavior. Therefore, to reduce the computational time, the foundation system was assumed to have an elastic characteristic. The parameters used to idealize this type of material model such as the concrete compressive strength (f_c), axial stiffness (EA), flexural rigidity (EI), unit weight of concrete, and Poisson's ratio (v) per unit length of the foundation system are shown in Table 3 (Abdulrazagh 2009).

To eliminate the effects of subgrade soil types and the slope of the trench walls on the analytical results of the minimum depth of cover, GW with a minor cohesion was selected for the engineered backfill from the soil group I of the CHBDC soil classifications CHBDC (2006) as a continuum media around the metal structures. A 0.3 m thick layer of ballast was also considered for both the 2D and 3D models. Therefore, in this study, the definition of *minimum depth of cover* also includes the depth of the ballast layer. In other words, the vertical distance between the lower level of sleepers and the crown is defined as the *depth of cover*. The behavior of the soil and ballast layers was defined as a nonlinear material based on the Mohr-Coulomb criterion. The soil and ballast specifications such as the type of material behavior, unit weight of soil (γ), Young's modulus (E_{ref} 2.07 × 10^4 to approximately 3.00 × 10^4 kN/m^2), Poisson's ratio, friction angle (ϕ), and cohesion (c) are shown in Table 4 (Abdulrazagh 2009).

The railway superstructure (rails and sleepers) was not idealized for the 2D analysis to simplify the calculations; however, it was idealized in the 3D analysis using PLAXIS 3D code because of its particular capabilities for modeling the longitudinal dimension of the structures and to obtain more accurate results by taking the lateral stiffness of the superstructure into account. To idealize the rail and sleepers in the 3D analyses, the properties of the UIC 60 rail type and the mono-block concrete sleepers were specified for the plate and soil type elements of the railway superstructure model, respectively (see Tables 5 and 6; Abdulrazagh (2009)). The rails and sleepers were modeled as linear elastic materials to eliminate the undesired behavior of the superstructure for

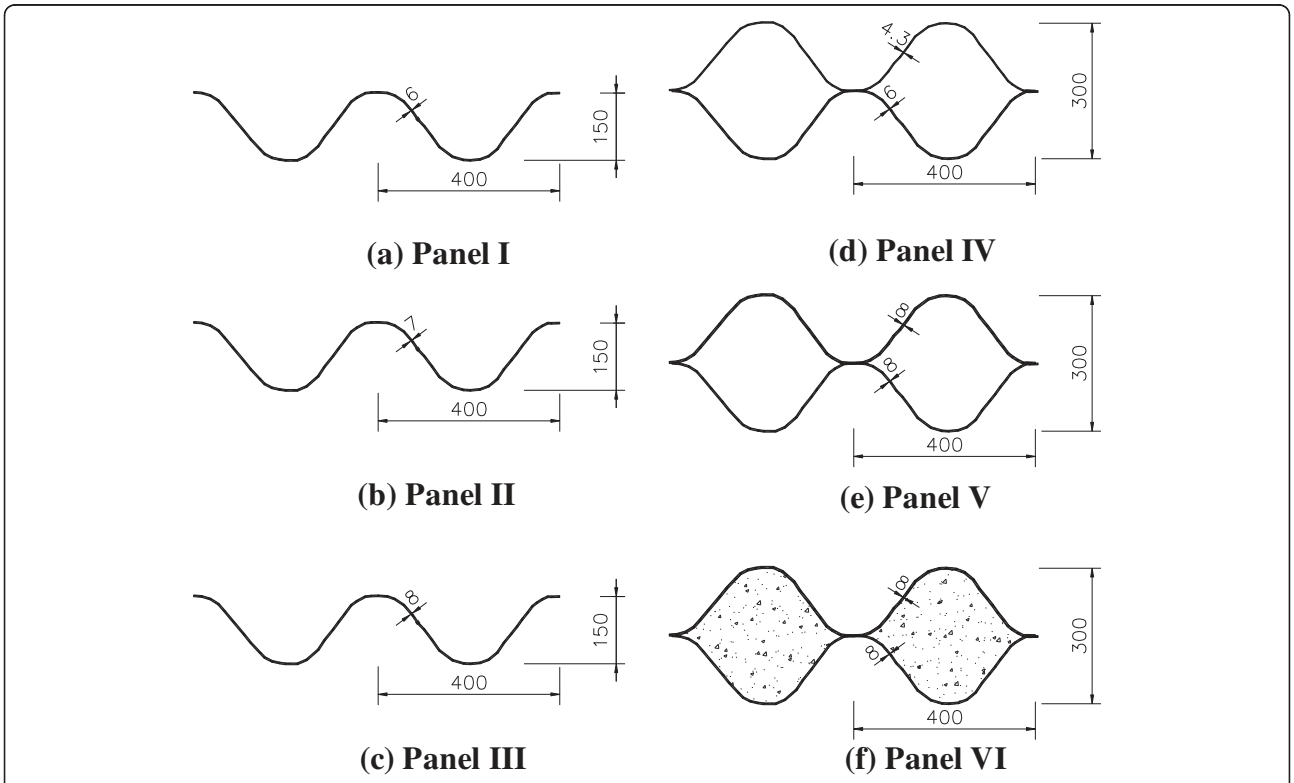

Figure 4 Types of conduit wall panels with dimensions in millimeters. (**a**) Standard 400 mm × 150 mm corrugation with 6-mm thickness, panel I. (**b**) Standard 400 mm × 150 mm corrugation with 7-mm thickness, panel II. (**c**) Standard 400 mm × 150 mm corrugation with 8-mm thickness, panel III. (**d**) Stiffened corrugated panel with 4.3-mm corrugated plate, panel IV. (**e**) Stiffened corrugated panel with 8-mm corrugated plate, panel V. (**f**) Stiffened corrugated panel with concrete filling, panel VI.

Table 2 Element specifications of conduit wall panels (corrugated steel plates)

Material model	Panel type	EA $\left(\frac{kN}{m}\right)$	EI $\left(\frac{kN.m^2}{m}\right)$	Poisson's ratio	M_p $\left(\frac{kNm}{m}\right)$	P_p $\left(\frac{kN}{m}\right)$
Elasto-plastic	I	1.65×10^6	4,630.80	0.3	117.30	2,478.00
Elasto-plastic	II	1.93×10^6	5,414.20	0.3	137.07	2,892.00
Elasto-plastic	III	2.18×10^6	6,151.80	0.3	155.67	3,270.00
Elasto-plastic	IV	2.81×10^6	20,846.29	0.3	226.71	4,218.00
Elasto-plastic	V	4.36×10^6	33,061.56	0.3	330.61	6,540.00
Elasto-plastic	VI	1.85×10^9	125,864.65	0.3	330.61	6,540.00

the determination of the minimum depth of cover for each analysis.

Loading model and loading pattern

The railway standard static loading pattern LM71 CEN (2002) that was used in the 2D and 3D FE analyses is shown in Figure 5. This loading pattern is also commonly used to design traditional railway bridges.

The factored loading diagram, which was directly applied to the 2D and 3D models, included the half magnitudes of those shown in Figure 5a,b (as a wheel load quantity). The longitudinal distributed loading model of LM71 (see Figure 5a) was selected for the 2D analysis to simplify the investigation of the moving effects of the railway load on the structure through a large amount of calculations in the numerical procedure. As an example, the factored strip loads of the 2D models are shown by AA and BB in Figure 6. The BB strip loads in Figure 6 for the 2D analyses were extended to boundaries.

Because the location of the railway moving load varies along the bridge, it is important to investigate the effects of the maximum lateral pressures, centric and eccentric loads on the foundation system, and crown and conduit walls. Therefore, the defined loading patterns in the 2D and 3D FE analyses were located in three critical locations as follows: (1) the right corner of the factored AA strip load for the 2D analysis (or the first right factored concentrated load for the 3D analysis) was located in line with the left foundation wall to study the stability of the structure against overturn moments and conduit wall buckling (Figure 6a, location 1); (2) the factored railway loading pattern was located symmetrically at the midspan to control the creation of a plastic hinge at the crown and at the conjunction points of the crown and haunches (Figure 6b, location 2); and (3) the right corner of the factored AA strip load in the 2D analysis (or the first right factored concentrated load in the 3D analysis) was located in line with the right foundation wall to investigate the eccentric loading effects on the analytical results (Figure 6c, location 3).

The initial measurements of the 2D and 3D idealization show that the railway location at the midspan defined by location 2 produced the maximum thrust in box and low-profile bridges. These measurements also show that the extension of the strip loads to the four sleepers adjacent to the outer sides of the spring line for location 2 in the 3D analysis results in a reasonable effective length for the longitudinal idealization of the railway track and consideration of the load effects (see Figure 7).

Definition of minimum cover governing criteria

For this study, the minimum cover for all of the cases in the numerical analysis is known as the cover depth, which creates three major modes of serviceability failure. First, by setting the minimum cover criterion, excessive uneven settlements in the railway bridge, which control the passenger comfort criteria, will be prevented (Neidhart 2005). Second, it prevents buckling in the various structural components. Once the settlement of the railway track does not exceed the permissible vertical deflection of the railway bridge, a buckling of the conduit wall, which results in soil tensile stresses, will not occur; however, the latter criterion was also checked by assigning nonlinear material properties to the wall conduits (Abdel-Sayed and Salib 2002). The third mode of failure, which controls the bearing capacity of the system as a type of foundation, is the soil local collapse. The mechanism of control for this type of failure was included in the numerical analysis by

Table 3 Element specifications of foundations and pedestals

Material	Material model	f_c $\left(\frac{kN}{m^2}\right)$	EA $\left(\frac{kN}{m}\right)$	EI $\left(\frac{kN.m^2}{m}\right)$	Unit weight $\left(\frac{kN}{m^3}\right)$	Poisson's ratio
Pedestal	Elastic	35,000	2.24×10^6	119,466.67	25	0.1
Foundation	Elastic	35,000	1.12×10^6	14.93×10^6	25	0.1

Table 4 Element specifications of soil and ballast

Material	Soil model	γ $\left(\frac{kN}{m^3}\right)$	E_{ref} $\left(\frac{kN}{m^3}\right)$	Poisson's ratio	φ	C_{ref} $\left(\frac{kN}{m^3}\right)$
Soil	Mohr-Coulomb	22	Increases 0.5×10^5 with every 1-m increase of depth	0.2	40°	7
Ballast	Mohr-Coulomb	20	2.07×10^4	0.2	40°	0

assigning the Mohr-Coulomb criterion to the soil material. These criteria will be discussed in more detail in the following subsections.

Permissible settlement of the railway track

For a soil-steel railway bridge, the minimum depth of cover must be defined in such a way to prevent the uneven settlements. In railway bridges, the criterion which restricts the settlement is related to speed of passing trains. According to CEN (2001) and the studies by Neidhart (2005), the settlement of the railway track δ satisfies the comfort criteria as:

$$\delta \leq 0.625 \frac{l^2}{V_{tr}^2}, \tag{1}$$

where V_{tr} is the running speed of the trains (in meters per second), and l is the distance between two points along the railway track where the differential settlement is desired (in meters). This equation results in a maximum allowable settlement (for a passing speed of 120 km/h) of about 62 mm at a distance equal to l (span/2) = 10.473 m. The permissible settlement for each of the predefined structures at a speed of 120 km/h (33.33 m/s) is shown in Table 7 (CEN 2001).

For this study and for the case of the railway bridge, the relative settlements between the spring line and midspan were checked for various depths of cover at different sections along the longitudinal axis of the bridge in the 3D FE analysis (at the sections of the embankment heel δ_{AB}, ballast heel δ_{CD}, sleeper edge δ_{EF}, outer edge of rail δ_{GH}, and axis of the railway track δ_{IJ} for the 3D analyses (see Figure 8) was compared to Equation 1. A similar approach was used in the 2D FE analysis to check the relative settlements between the spring line and midspan at the x and y plane (δ_{AB}).

To satisfy the serviceability of the railway bridge, the vertical deformation of analytical bridge should be less than the permissible settlement defined in Table 7. In other words, if a specific soil cover depth satisfies all of the aforementioned relative settlements at the same time, then it is defined as the *minimum depth of soil cover* for a specific structure. This depth was checked for each of the structures.

Buckling control in the conduit walls

The strength required for the service life of the soil-steel bridge to avoid the buckling of the conduit wall is controlled by the combined bending moment and axial thrust as follows (CSPI and AISI 2002):

$$\alpha = \left(\frac{P}{P_{pf}}\right)^2 + \left|\frac{M}{M_{pf}}\right| \leq 1, \tag{2}$$

where P and M are the axial thrust and bending moments due to the dead load and railway load in conduit walls, and they are calculated using the 2D or 3D FE analyses. P_p and M_p are the compressive strength and plastic moment capacity of the predefined conduit wall sections, respectively, and are shown in Table 2 and Figure 4.

This criterion was automatically controlled by defining an elasto-plastic behavior for the conduit walls as beam elements for the 2D FE analysis. As the dead and live loads in the 3D FE analysis cause axial thrusts and bending moments at both the x-y plane (P_{11} and M_{11}) and the x-z plane (P_{22} and M_{22}) so Equation 2 should be controlled in both directions. More details of the buckling control in both planes are presented in the following sections. However, the initial investigations of the different 3D models revealed that the axial thrusts and bending moments at the x-y plane (cross section) are dominant to the x-z plane values, so they control the buckling of the structures.

Control of the soil body failure

For the soil-steel bridges, the soil above the conduit is prone to shear failure if the embankment is subjected to loads that are eccentric with respect to the conduit axis. An insufficient depth of cover results in a local soil

Table 5 Element specifications of rails

Material	Material model	E $\left(\frac{kN}{m^2}\right)$	EA $\left(\frac{kN}{m}\right)$	EI $\left(\frac{kN.m^2}{m}\right)$	Unit weight $\left(\frac{kN}{m}\right)$	Poisson's ratio
Rail	Elastic	2.0×10^8	1,517,400	6,110	0.6034	0.25

Table 6 Element specifications of concrete sleepers

Material	Material model	γ $\left(\frac{kN}{m^3}\right)$	E_{ref} $\left(\frac{kN}{m^2}\right)$	K_0	Poisson's Ratio
Sleeper	Elastic	25	2.8×10^7	-	0.1

failure, which fundamentally arises in the presence of tensile or shear stresses over the maximum allowable stress defined by the Mohr-Coulomb criterion (Abdel-Sayed and Salib 2002; Lee 2002; Beben 2009; Flener 2010). This type of failure was a 'non-converged deformation' during the reconstruction of elasto-plastic stiffness matrix which was automatically controlled by the software as the soil body failure during the setting of the acceptable soil cover on the structure in the numerical analysis.

Results and discussion

Numerical results

In this section, the 2D and 3D FE numerical results are discussed, and the developmental procedure of the interpolation equations is described.

Results of the 2D finite element analyses

A comparison between the results of the 2D analysis for box and low-profile arches is shown in Figure 9.

As a result of the various numerical analyses and satisfying the aforementioned criteria, the minimum depth of cover was evaluated against the span of railway box and low-profile arch bridges using various panel types (stiffness) and with respect to the permissible settlement criterion. A brief review of these data demonstrates that the trends of the minimum depth of cover for box bridges differ from that of the low-profile arches. This is due to the different structural geometry of the boxes which results in a different mechanism of behavior under load. Thus, to ease the process of finding the new pattern of minimum depth of cover, the data have been separately categorized for boxes and low-profile arches in the following step.

Regarding the power trend type of the CHBDC formula of minimum depth of cover $D_h/6((D_h/D_v)^{0.5})$ and the trend of changes in the cover depth for the boxes and low-profile arches versus the span, exponential, polynomial, or power trend lines were assumed to properly fit to the data of 2D results. Therefore, two types of exponential, one type of polynomial, and one type of power trend line were examined as follows: (1) exponential trend line as a function of the effective span (D_h); (2) power trend line as a function of the effective span (D_h); (3) exponential trend line as a function of D_h/D_v (D_v effective rise of the structure); and (4) polynomial trend line as a function of D_h/D_v. A comparison of the R^2 values of the trend lines shows that the exponential and power functions of D_h represent a more accurate estimation of the data. However, due to the dimensions of the formulas for calculating the minimum depth of cover that must be in meters, an exponential function (D_h) was chosen to describe the change in the minimum depth of cover versus the effective span.

In order to account for moment of inertia and length of span which are the representative of relative stiffness of backfill and culvert structure and the geometry of metal culver structure, the basic form of the minimum depth of cover resulted from 2D analysis for the railway boxes and high-profile arches is introduced as follows:

$$H_{\min} = \alpha\left(N_f\right)^{\beta} e^{\mu D_h}, \tag{3}$$

where the dimensionless ratio N_f is defined by the following:

$$N_f = \frac{E_s {D_h}^3}{EI}, \tag{4}$$

in which E_s is the secant modulus of the backfill, which depends upon the quality and compaction of backfill and the depth of cover; E is the modulus of elasticity of the corrugated plates; and I is the moment of inertia of

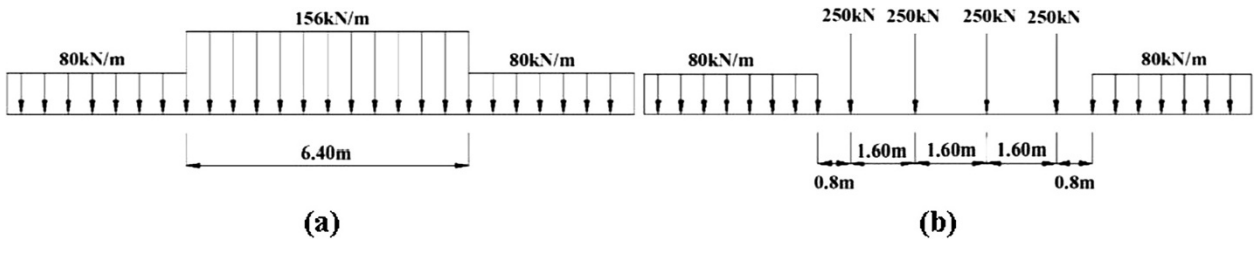

Figure 5 Eurocode model LM71 railway bridge loading diagram. (**a**) Longitudinal distribution of the unfactored axle loads used in 2D FE models. (**b**) Unfactored loading diagram used in 3D FE models (CEN 2002).

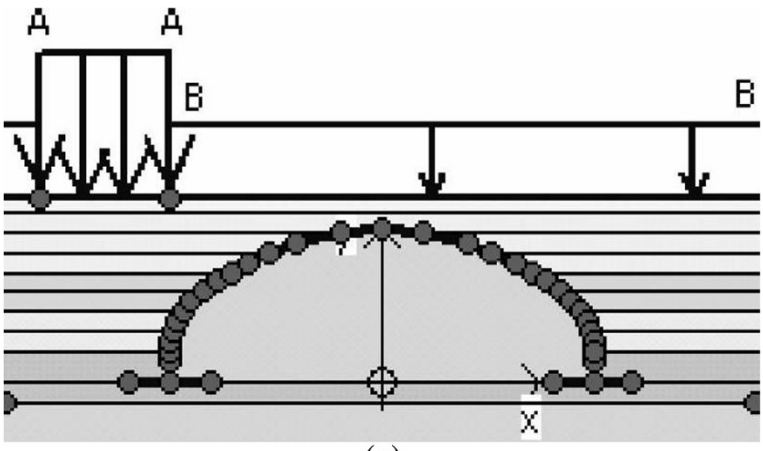

(a)

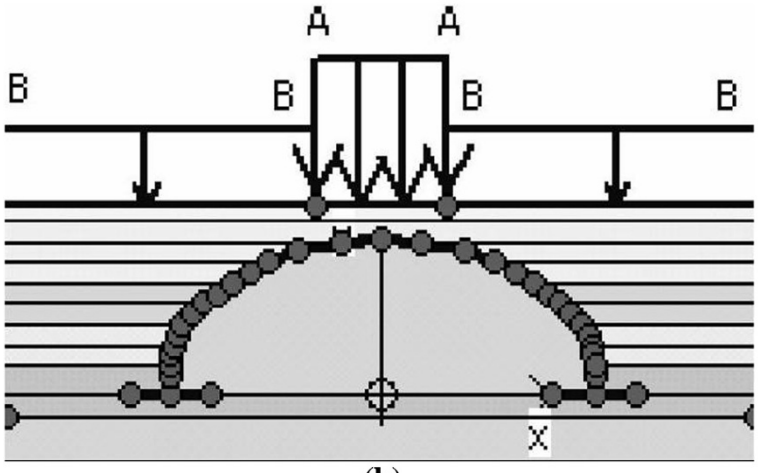

(b)

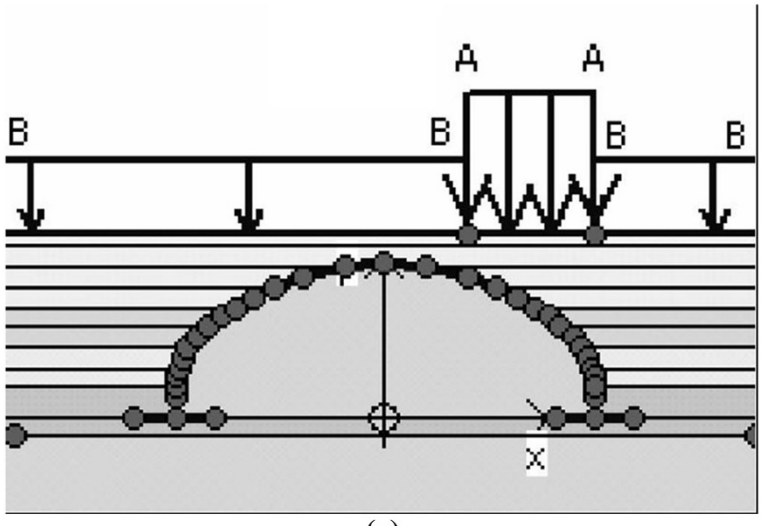

(c)

Figure 6 Location of factored railway load. (**a**) The right corner of factored AA strip load in 2D analysis located in line with the left foundation wall (location 1). (**b**) The factored railway loading pattern located symmetrically on midspan (location 2). (**c**) The right corner of factored AA strip load in 2D analysis located in line with right foundation wall (location 3).

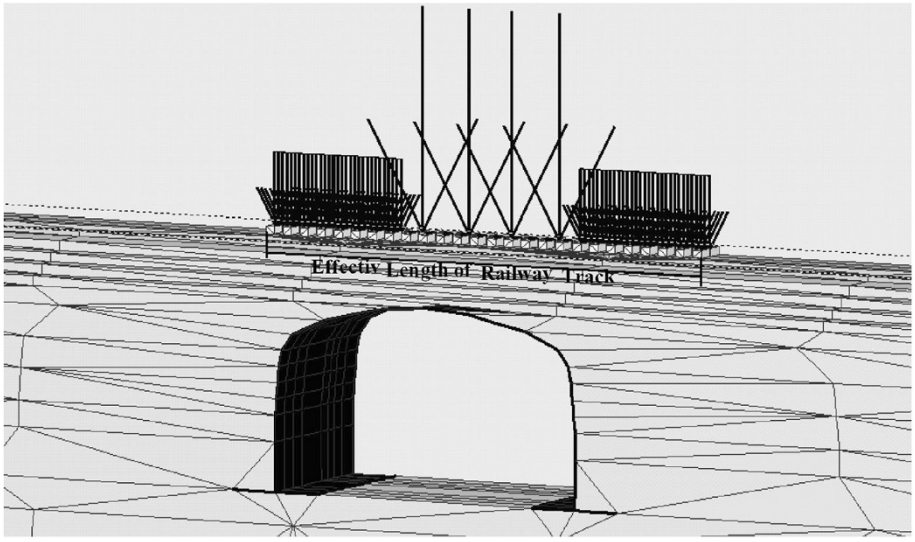

Figure 7 Effective length for longitudinal idealization of railway track in 3D FE analyses.

the conduit wall per unit length of the bridge. Variables α, β, and μ in Equation 3 are unknown constants. These constants were calculated separately for the boxes and low-profile arches using the least-squares method to determine the function of best fit. The final set of parameters is listed below:

$$\begin{cases} \alpha = 0.0139 \\ \beta = 0.25 \\ \mu = \dfrac{1}{3} \end{cases} \quad \text{BOX} \qquad \begin{cases} \alpha = 0.0139 \\ \beta = 0.25 \\ \mu = \dfrac{1}{3} \end{cases} \quad \text{LPA.}$$

By substituting the above parameters into Equation 3, the equations for the minimum depth of cover are given by Equations 5 and 6, assuming that all the metal structures are buried in GW with 24 MPa of secant elasticity modulus as an average value in the mid-height of the structure:

$$H_{\min} = 0.0139 {N_f}^{0.25} e^{D_h/3} \quad R^2 = 0.90 \text{ for boxes,} \tag{5}$$

$$H_{\min} = 0.0100 {N_f}^{0.25} e^{D_h/7} \quad R^2 = 0.87 \text{ for low-profile arches.} \tag{6}$$

As shown in the above equations, the R^2 values are close to 1.0, which represents the considerable accuracy of the interpolation function with minimal divergence from the 2D FE numerical results. Regarding the maintenance operations, buckling criterion, and AASHTO and CHBDC limits, a recommended minimum of 0.6 m and maximum of 1.5 m must be maintained for the depth of cover using the following expressions:

$$H_{\min} = \min \begin{cases} 1.5\ m \\ \max \begin{cases} 0.6\ m \\ H = 0.0139 \left(\dfrac{E_s {D_h}^3}{EI} \right)^{0.25} e^{D_h/3} \end{cases} \end{cases} \text{for boxes,} \tag{7}$$

$$H_{\min} = \min \begin{cases} 1.5m \\ \max \begin{cases} 0.6m \\ H = 0.0100 \left(\dfrac{E_s {D_h}^3}{EI} \right)^{0.25} e^{D_h/7} \end{cases} \\ \text{for low-profile arches,} \end{cases} \tag{8}$$

The results of the 3D finite element analysis for control of buckling

Checking the applicapability of the 2D-based equations of minimum cover in practical three-dimensional problems, a series of three-dimensional FE analyses were carried out to control the out-of-plane buckling in the steel plates due to three-dimensional pattern of the train

Table 7 Permissible settlement at speed 120 km/h

Structure type	Span (m)	*l* (m)	$\delta_{permissible}$ (mm)
Box culvert	8.074	4.035	9.00
	10.514	5.255	15.00
	11.023	5.511	17.00
	13.456	6.728	25.00
Low-profile arch	14.130	7.065	28.00
	16.518	8.259	38.00
	20.946	10.473	62.00
	23.405	11.702	77.00

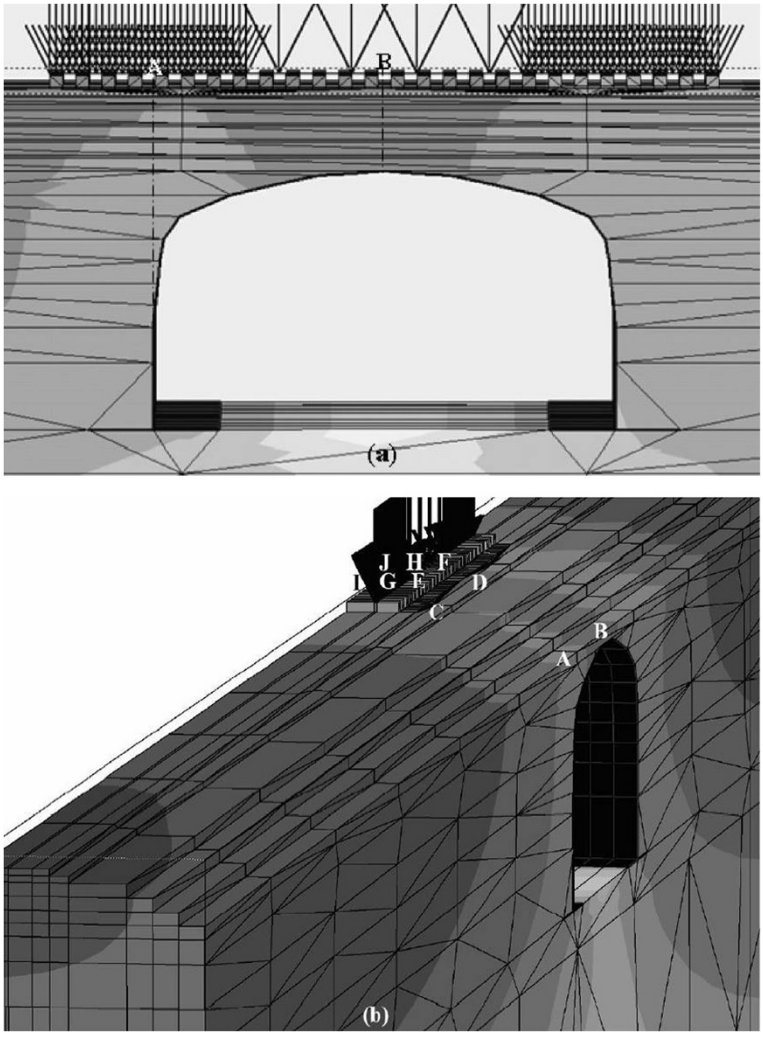

Figure 8 Points to be studied in tension of spring line and mid-span. It is for the measurement of relative settlements in box bridges: (**a**) at *x-y* plane and (**b**) along the longitudinal dimension of the bridge.

loads. In this regard, the combination of thrusts and bending moments are checked using Equation 2 at two different sections (under rail and in the middle of track) in the midspan (points G and I in Figure 8b) and at in tension of spring line (points H and J in Figure 8b). The results of buckling control (α) for panel VI are illustrated in Figure 10. This figure shows that the combination of thrusts and bending moments in both planes ($\alpha_{x\text{-}y}$ and $\alpha_{y\text{-}z}$) are quite smaller than the maximum limitation of $\alpha_{\text{allowable}} = 1.0$. Also, this figure shows that $\alpha_{x\text{-}y}$ is always greater than $\alpha_{y\text{-}z}$ which means that the out-of-plane bending does not control the buckling behavior of the steel plates. The comparison between Figure 10a,b shows that the buckling under the rail and in the middle of track has almost similar values.

As can be seen in Table 8 for the structures with wall stiffness less than those of panel VI, in order to withstand under railway loads, the height of cover has significantly increased. To make a decision on the best alternative for bridge construction from the design aspect, a technical and economical comparison should be made between two different cases: the bridges with the small stiffness and high depth of cover and the bridges with the high stiffness and shallow depth of cover considering the limitation of the vertical project level (for optimizing the earth work in the project). However, none of the cases show an $\underline{\alpha}$ value greater than 1.0.

In summary, the results of Figure 10 and Table 8 show that the out-of-plane bending ($\alpha_{y\text{-}z}$) does not control the buckling behavior of the steel plates. Thus, the proposed equations for minimum depth of cover can be appropriately used for practical purposes.

Discussion

The results of the 2D FE analyses are compared to the standard codes, and the newly proposed equations as

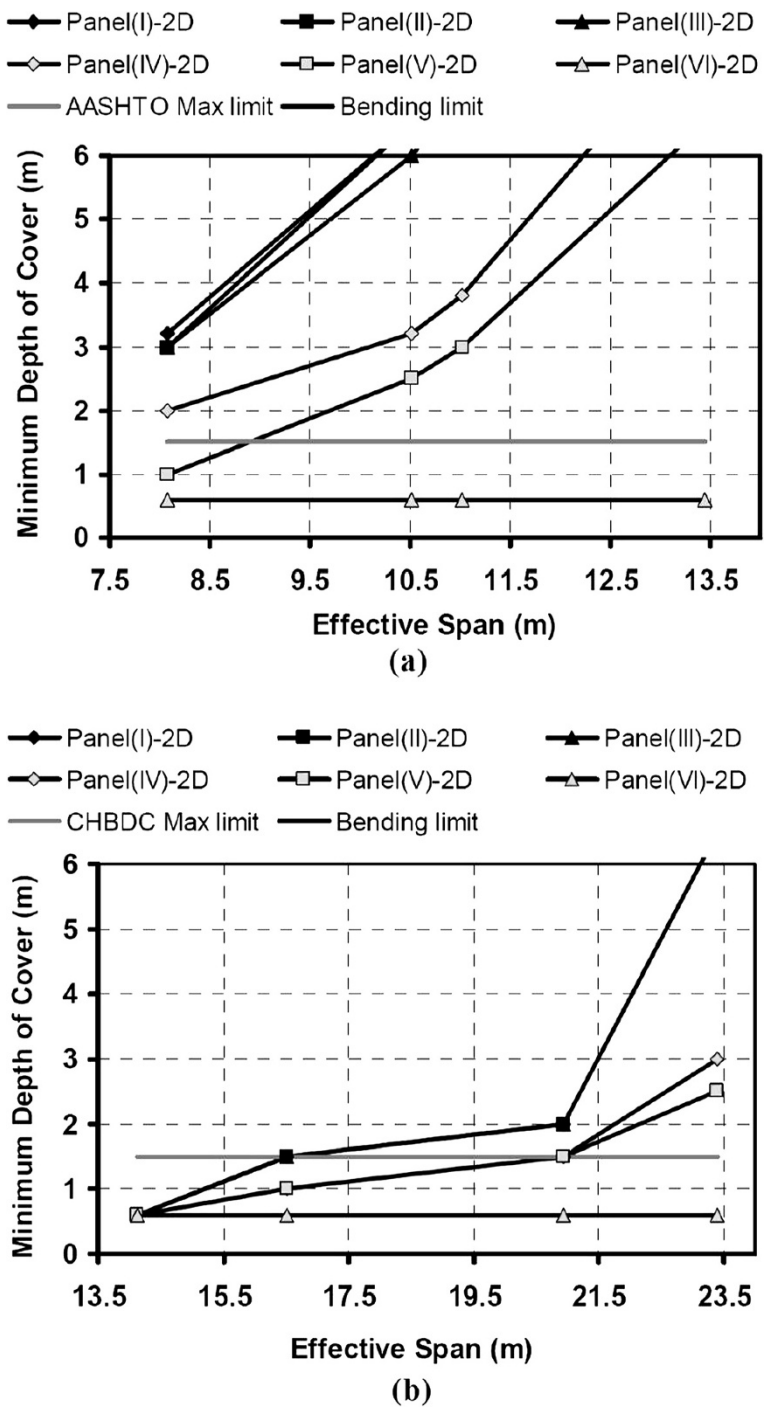

Figure 9 The comparison of 2D results for (a) box bridges and (b) low-profile arches.

well as the validity limit of these formulas are discussed in the following subsections.

Validity range of the derived equations

The results of the 2D FE analyses are compared to the values of the proposed box equations (referred to as the *formula* in the legends) and the *AASHTO limit* are shown in Figure 11. There is good agreement between the 2D FE results and the values of Equation 5. The conformity of Equation 5 with the 2D results was evaluated using an R^2 value that was calculated using $R^2 = 1 - \mathrm{SSE/SST}$, where $\mathrm{SSE} = \Sigma \left(Y_i - \hat{Y}_i\right)^2$ and $\mathrm{SST} = (\Sigma\, Y_i^2) - ((\Sigma Y_i)^2)/n$. The R^2

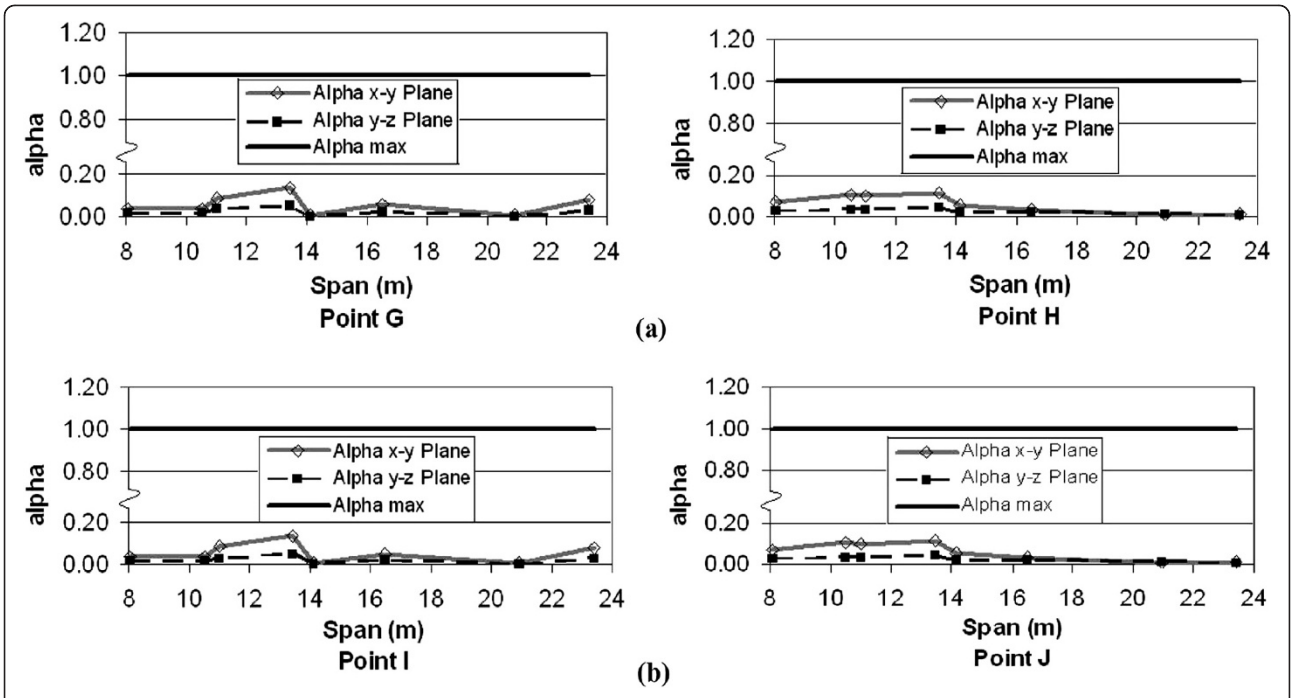

Figure 10 Control of buckling for structures with panel VI: (a) Under the rail. (**b**) In the middle of track.

value for this equation was calculated to be 0.90, which demonstrates a reasonable agreement with the 2D results.

It should be noted that an equation is not given in the CHBDC and AASHTO for the minimum depth of cover of box culverts. Only a minimum of 0.3 m and a maximum of 1.5 m are specified in the CHBDC (2006) and AASHTO Highway Bridges (2000), respectively. By accounting for the buckling criterion of the railway box bridges, a minimum of 0.6 m (called the *bending limit*) was obtained for the depth of cover, which is indicated by the dashed lines in Figure 11.

Figure 11a shows that panels IV and V with a span of 8.07 m and panel VI for all of the spans follow the

Table 8 Control of buckling for the structures with profiles other than panel VI

Span (mm)		Points G and I				Points H and J			
		Panel I	Panel III	Panel IV	Panel V	Panel I	Panel III	Panel IV	Panel V
Box	8.07	6.0 m[a]				6.0 m[a]			
		0.157[b] 0.153[c]				0.689[b] 0.687[c]			
	10.51	-	6.5 m[a]				6.5 m[a]		
			0.297[b] 0.294[c]				0.730[b] 0.719[c]		
	11.02	-		6.5 m[a]				6.5 m[a]	
				1.118[b] 0.105[c]				0.873[b] 0.857[c]	
	13.46	-			6.5 m[a]				6.5 m[a]
					0.134[b] 0.131[c]				0.984[b] 0.976[c]
LPA	14.13	0.6 m[a]				0.6 m[a]			
		0.543[b] 0.540[c]				0.490[b] 0.485[c]			
	16.52	1.5 m[a]				1.5 m[a]			
		0.333[b] 0.279[c]				0.829[b] 0.821[c]			
	20.95	2.0 m[a]				2.0 m[a]			
		0.490[b] 0.434[c]				0.552[b] 0.506[c]			
	23.40	6.5 m[a]				6.5 m[a]			
		0.494[b] 0.491[c]				0.903[b] 0.887[c]			

[a] Depth of cover; [b] $\alpha_{x\text{-}y}$; [c] $\alpha_{y\text{-}z}$.

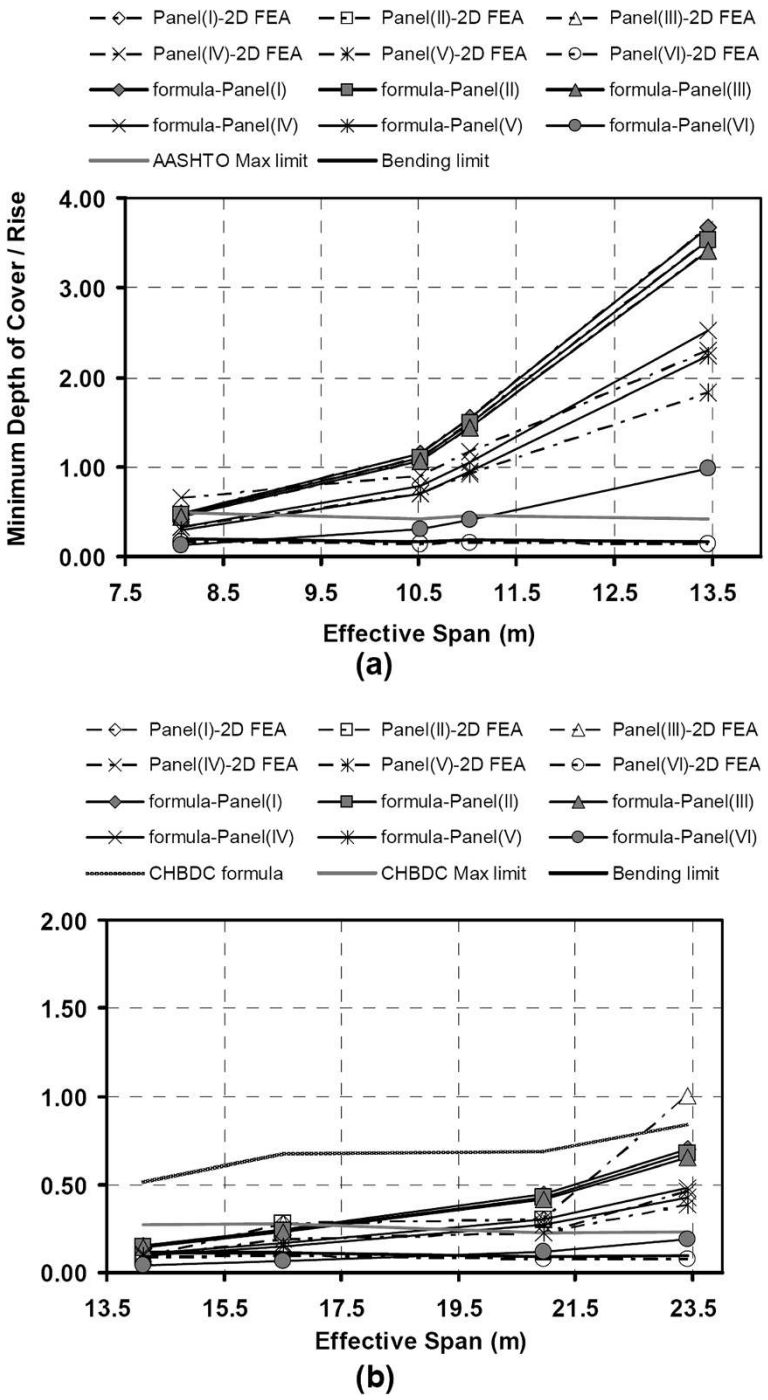

Figure 11 Results of 2D FE analyses in comparison with two values. (**a**) Box formula and the AASHTO limit. (**b**) LPA formula and the CHBDC limit.

AASHTO max limit. The figure also presents that the agreement between the 2D FE results and the values of Equation 5 is good for all panels (R^2 = 0.90) specially panels IV to VI. The results of 2D FE analysis for panels I to III are not shown in this figure because of the high value of minimum depth of cover. In these cases, usually stiffer panels are used to reduce the required minimum cover depth.

The results of the 2D FE analysis are compared to the values of the proposed low-profile arch equation (referred to as the *formula* in the legends), and the *CHBDC max limit* and the *bending limit* (0.6 m for the low-

Table 9 The R^2 values for 2D equations for all spans

Panel type	Box	LPA
I	0.91	0.83
II	0.92	0.87
III	0.93	0.88
IV	0.98	0.97
V	0.96	0.98
VI	-	-

profile arches) are illustrated in Figure 11b. The R^2 value of 0.87 for Equation 6 demonstrates a reasonable agreement with the 2D FE results.

The values of the minimum depth of cover specified by the CHBDC are also shown in Figure 11b. The CHBDC recommends using the greater of $D_h/6((D_h/D_v)^{0.5})$ and 1.5 m for non-stiffened panels Hafez and Abdel-Sayed (1983). A comparison between the *CHBDC formula* and the resulting data shows that the minimum depth of cover specified by the CHBDC is much higher than those obtained from 2D FE analyses (without considering the 0.6-m limit). This difference may refer to the recommendation of more conservative values by the standards, so the recommended values should be applicable for all practical conditions. Figure 11b shows that the panel IV with the span of 16.52 m, panel V with the span of 16.520 and 20.95 m, and panel VI for all of the spans follow the *CHBDC max limit.*

The overall conformity of the newly established equations obtained from the 2D FE analysis was discussed in the previous section. However, to investigate the validity of the newly established formulas with respect to the panel types, the R^2 value was calculated separately for each type of panel. The R^2 values are shown in Table 9.

From the results shown in the table, the equations are applicable for panels I to V for boxes and low-profile arches because the R^2 values are greater than 0.85. It is recommended to use the equations conservatively for panel VI or to use the minimum value of 0.6 m for the depth of cover. The results of the 2D FE analysis for panel VI represented a depth of cover less than 0.6 m. A minimum of 0.6 m must be maintained for the *CHBDC minimum* (*bending*) *limit*.

Conclusions

The minimum depth of cover requirements given by different codes are typically based on vehicle loads, non-stiffened panels, and only the geometrical shape of the metal structure to avoid the failure of soil cover above a soil-steel bridge. In this paper, the effects of spans larger than 8 m (using stiffened panels under railway loads) are investigated using an FE analysis. For this study, 2D and 3D FE analyses of four low-profile arches and four box culverts with spans larger than 8 m were performed to develop new patterns for the minimum depth of soil cover. Using the least-squares method to adopt the best-fit equation of the numerical data, two new sets of formulas were recommended. Based on the numerical results, the primary research findings are summarized as follows:

1. The minimum depth of cover increases exponentially along with an increase in the span of boxes and low-profile arches.
2. The increase of rigidity of the wall panels significantly decreases the depth of cover required above the bridges. The efficiency of the stiffened panels is more pronounced for large spans.
3. Different trends of the minimum depth of cover were determined for box bridges and low-profile arches. This difference is due to the various structural geometries of the boxes that resulted in a different mechanism of behavior under load.
4. Exponential forms of the minimum depth of cover for railway boxes and low-profile arches were developed as a function of the span and relative stiffness of the backfill and the culvert structure, which exhibited good conformity with the 2D FE analysis results ($R^2 > 0.85$).
5. A survey on the validity limit of the new formulas established from the 2D FE analyses demonstrated that the equations are appropriate to calculate the minimum depth of cover for all of the boxes and low-profile arches with spans greater than 8 m with stiffened and non-stiffened panels. However, a minimum depth of cover of 0.6 m must always be maintained.

Competing interests

The authors declare that they have no competing interests.

Authors' contributions

As corresponding author, ME defined the main theme and objective of the study for PHA, explained the research methodology, processed the obtained numerical results, and guided the calculation of closed form equations for minimum soil cover on selected bridges. ME was involved in language editing and finalizing the manuscript writing. JAZ edited the first draft of the paper and controlled the obtained numerical results. PHA accomplished the whole of the numerical simulations and prepared the first draft of the paper. All authors read and approved the final manuscript.

Authors' information

ME is an assistant professor at the School of Railway Engineering in IUST. JAZ is an associate professor at the School of Railway Engineering in IUST. PHA is a PhD candidate at the University of Tehran.

Author details

[1]School of Railway Engineering, Iran University of Science and Technology, University Street, Hengam Aveneu, Narmak, Tehran 1684613114, Iran. [2]School of Civil Engineering, University of Tehran, Tehran 111554563, Iran.

Received: 18 September 2012 Accepted: 13 February 2013
Published: 20 March 2013

References

Abdel-Sayed G, Salib SR (2002) Minimum depth of soil cover above soil-steel bridges. J Geotech Geoenviron Eng ASCE 128(8):672–681
Abdel-Sayed G, Bakht B, Jaeger LG (1993) Soil-steel Bridges, Design and Construction. McGraw-Hill Pub, New York
Abdulrazagh PH (2009) 2D and 3D Finite element analysis of railway soil-steel bridges with attitudes towards minimum depth of soil cover. Iran University of Science and Technology, M.Sc. Thesis
ARTC (2005) Buried Corrugated Metal Structures. Australian Rail Track Corporation, Adelaide
ASTM (1982) A796/A796M: Standard Practice for Structural Design of Corrugated Steel Pipe, Pipe-Arches, and Arches for Storm and Sanitary Sewers and Other Buried Applications. ASTM International, West Conshohocken, PA
Beben D (2009) Numerical analysis of soil-steel bridge structure. Baltic J Road & Bridge Eng 4(1):13–21
CALTRANS (2000) Bridge Design Specifications. California Transportation Board, Sacramento, CA
CEN (2001) EN1990 Eurocode: Basis of Structural Design. Draft Annex A2: Application for Bridges (Normative). European Committee for Standardization, Brussels
CEN (2002) Eurocode 1: Actions on Structures Part 2 - Traffic Loads on Bridges (prEN 1991–2). European Committee for Standardization, Brussels
CHBDC (2006) CAN/CSA-S6-06 Section 7: Buried Structures. National Standard of Canada, CSA International, Ontario
CSPI and AISI (2002) Handbook of Steel Drainage & Highway Construction Products, 2nd edn. American Iron and Steel Institute, Washington DC
DMRB (2001) Design of corrugated steel buried structures with spans greater than 0.9 meters and up to 8.0 meters: BD12/01, vol. 2, section 2, part 6. British Design Manual for Roads and Bridges, London
Duncan JM (1979) Behavior and design of long-span metal culverts. J Geotech Eng Division ASCE 105(3):399–418
El-Sawy KM (2003) Three-dimensional modeling of soil-steel culverts under the effect of truckloads. J Thin-Walled Struct 41:747–768
Flener EB (2010) Testing the response of box-type soil-steel structures under static service loads. J Bridge Eng ASCE 15(1):90–97
Flener EB, Karoumi R (2009) Dynamic testing of a soil-steel composite railway bridge. J Eng Struct 13(12):2803–2811
Flener EB, Karoumi R, Soundquist H (2005) Field testing of a long-span arch steel culvert during backfilling and service. J Struct Infrastruct Eng 1(3):181–188
Hafez H (1981) Soil-steel structures under shallow cover. PhD dissertation. University of Windsor
Hafez H, Abdel-Sayed G (1983) Soil failure in shallow covers above flexible conduits. Can J Civil Eng 10:654–661
Highway Bridges AASHTO (2000) Soil-Corrugated Metal Structure Interaction Systems, 2nd edn. American Association of States Highway and Transportation, Washington, DC
Lee J (2002) The performance of soil-steel bridges with shallow soil cover under vehicle load. Proceedings 5th Int Conf on Bridge Maintenance. Saf Manage 1:42–50
MacDonald L (2010) Numerical modelling of vehicle loads on buried orthotropic steel shell structures. Dalhousie University, M.Sc Thesis
Manko ZZ, Beben D (2005) Research on steel shell of a road bridge made of corrugated plates during backfilling. J Bridge Eng ASCE 10(5):592–603
Manko ZZ, Beben D (2008) Dynamic testing of a corrugated steel arch bridge. Can J Civil Eng 35(3):246–257
Mohammed H, Kennedy JB, Smith P (2002) Improving the response of soil-metal structures during construction. J Bridge Eng ASCE 7(1):6–13
Neidhart TH (2005) True-to-scale *in situ* tests determining dynamic performance of earthworks under high speed train loading. Geotechnics Roads 1:27–34
OHBDC [Ontario Highway Bridge Design Code] (1992) Buried Structures, 3rd edn. Ontario Ministry of Transportation, Toronto
Peck OK, Peck RB (1984) Experience with flexible culverts through railroad embankments. Proc 2nd Int Conf on Soil Mechanic Found Eng 2:89–98
Peterson DL, Nelson CR, Li G, McGrath TJ, Kitane Y (2010) Recommended design specified for live load distribution to buried structures. NCHRP Report 647. Transportation Research Board, Washington
Planning and Budget Organization (1985) Code 88 Criteria of Geometrical Design of Roads and Crossings. Planning and Budget Organization, Tehran

doi:10.1186/2008-6695-5-7
Cite this article as: Esmaeili *et al.*: **Minimum depth of soil cover above long-span soil-steel railway bridges.** *International Journal of Advanced Structural Engineering* 2013 **5**:7.